

Theoretical analysis of localized heating in human skin subjected to high voltage pulses

Gregory T. Martin, Uwe F. Pliquet¹, James C. Weaver^{*}

Harvard–MIT Division of Health Sciences and Technology, Massachusetts Institute of Technology, 16-316, Cambridge, MA 02139, USA

Received 11 September 2000; received in revised form 14 November 2001; accepted 28 November 2001

Abstract

Electroporation, the increase in the permeability of bilayer lipid membranes by the application of high voltage pulses, has the potential to serve as a mechanism for transdermal drug delivery. However, the associated current flow through the skin will increase the skin temperature and might affect nearby epidermal cells, lipid structure or even transported therapeutic molecules. Here, thermal conduction and thermal convection models are used to provide upper and lower bounds on the local temperature rise, as well as the thermal damage, during electroporation from exponential voltage pulses (70 V maximum) with a 1 ms and a 10 ms pulse time constant. The peak temperature rise predicted by the conduction model ranges from 19 °C for a 1 ms time constant pulse to 70 °C for the 10 ms time constant pulse. The convection (mass transport) model predicts a 18 °C peak rise for 1 ms time constant pulses and a 51 °C peak rise for a 10 ms time constant pulse. The convection model compares more favorably with previous experimental studies and companion observations of the local temperature rise during electroporation. Therefore, it is expected that skin electroporation can be employed at a level which is able to transport molecules transdermally without causing significant thermal damage to the tissue. © 2002 Published by Elsevier Science B.V.

Keywords: Electroporation; Local heating; Temperature rise; Thermal model; Human skin; Transdermal drug delivery

1. Introduction

Controlled, transdermal delivery of therapeutic agents is potentially of major clinical importance. This process requires an increase in skin permeability such that a sufficient amount of drug may be transported in a controlled fashion. Electroporation, which can increase the permeability of bilayer lipid membranes in the *stratum corneum* (SC) using high voltage pulses, has potential as a mechanism for transdermal drug delivery.

Despite the number of studies that investigate the application of electroporation to transdermal drug delivery [1–4], very little attention has been given to the thermal effects that may be caused by these high voltage pulses. A voltage pulse causes an associated current flow through the skin, which due to its finite electrical resistance, will increase the local skin temperature through electrical dissipation (Joule heating). This local temperature rise may affect: (1) the barrier

function of the skin if the temperature rise causes a phase change in the SC lipids and/or a denaturation of SC proteins; (2) the local morphology of the skin structure if the heating causes water to vaporize; and (3) the therapeutic molecules destined for transdermal drug delivery. Further, if nearby epidermal tissues experience a prolonged temperature rise beyond a threshold, damage may result. It is the purpose of the present theoretical study to model and investigate the magnitude of the temperature rise within skin during electroporation and to assess the potential thermally mediated effects.

2. Materials and methods

The skin's barrier function is mainly afforded by the stratum corneum (SC), a multi-lamella structure within the first ~ 20 µm of the skin surface. This structure exhibits a very high electrical resistance and an extremely low permeability to transport. Thus, an electric field applied across skin will concentrate mainly within the SC. Depending on the pulse duration, an electric “breakdown” is likely to occur if the voltage across the SC is about 50–100 V. During this

^{*} Corresponding author. Tel.: +1-617-253-4194; fax: +1-617-253-2514.

E-mail address: jim@geldrop.mit.edu (J.C. Weaver).

¹ Present address: Faculty of Chemistry/PCIII, University of Bielefeld, D-33615 Bielefeld, Germany, Tel.: +49-521-106-6261.

breakdown, the resistance of the SC, R_{SC} , decreases by up to four orders of magnitude within less than a microsecond [5]. The electric breakdown of skin shows a high localization, where the drop in R_{SC} occurs in a local dissipation region (LDR) [6–8]. The drop in R_{SC} is accompanied by an increase in the skin permeability to small ionic species (Na^+ , Cl^- , etc.), which are responsible for most of the current flow. Our hypothesis is that the decrease in electrical and transport resistance is the result of electroporation that creates aqueous pathways through the lipid bilayers within the SC. Molecules are transported through these pathways by driving potentials such as local electrophoresis, pressure gradients, diffusion, electro-osmosis and/or osmotic gradients. The transport of charged, fluorescent molecules during electroporation has been found to take place in a limited region, usually in the center of the LDR, which is called the local transport region (LTR) [5–8].

It is believed that during electroporation, the smallest, newly created aqueous pathways have an effective hydrodynamic radius of about 1 nm and involve about 0.1% of the total skin area [2,9,10]. The newly created pathways are concentrated within regions (LDRs), which typically cover about 10% of the electrically exposed skin surface. Thus, the fractional area, $F_{w,ions}$, within the LDRs which is occupied by aqueous pathways is about 1%.

In order to simplify the model and the analysis, we average over the individual pathways and treat the LDR as a continuum. The electrical and thermal properties of the LDR are estimated by weighting the electrical and thermal properties of saline and lipid in proportion to the fractional aqueous area within the LDR. This provides a description on a spatial scale that is larger than a single aqueous pathway, but nevertheless is appropriate for estimating the temperature rise in the LDR. Fig. 1 shows a schematic

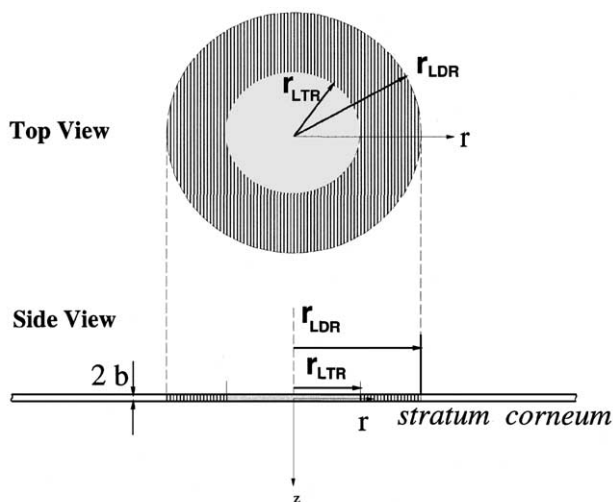


Fig. 1. Schematic diagram of local transport region (LTR) within a local dissipation region (LDR) formed in the stratum corneum during electroporation.

diagram of the SC geometry and Fig. 2 shows a schematic for the model of molecular, electrical and heat transport.

2.1. Electrical model

Heat in the LDR and in the surrounding medium is generated by the dissipative conversion of electrical energy to thermal energy (Joule heating). Thus, the heat generation distribution is dependent on the electric field and it is therefore necessary to first model the current flow. Due to the fact that the electrical resistivity of SC is much greater than that of saline ($\rho_{SC} = 1 \text{ M}\Omega \text{ m} \gg \rho_{saline} = 0.72 \Omega \text{ m}$, [13], it is assumed that the unelectroporated SC is electrically insulating. Therefore, all the current flows through the SC by way of the aqueous pathways in the LDR's, created by electroporation. In addition, heat is generated in the nearby epidermis and in the saline surrounding the LDR owing to the spreading resistance [11]. Spreading resistance occurs because current flows from an effectively infinite distance through the LDR, which has a finite (and small) radius.

A single LDR, therefore has the resistance:

$$R_{LDR} = \frac{2b\rho_{LDR}}{\pi r_{LDR}^2} \quad (1)$$

$$\rho_{LDR} = \frac{\rho_{saline}}{F_{w,ions}} \quad (2)$$

where r_{LDR} is the radius of the LDR, $2b$ is the thickness of the SC, and ρ_{LDR} is the bulk and effective resistivity of the LDR, which is determined from the fractional aqueous area of the LDR ($F_{w,ions} \sim 1\%$) and the saline resistivity.

In the epidermis and in the external fluid, electrical energy is dissipated by the spreading resistance. It is assumed that the LDR surfaces in contact with the epidermis and with the external fluid are equipotentials. At a far distance above the SC, the potential is set at $U(t)$ and at a far distance below the SC, the potential is set to ground. The total spreading resistance in the saline and in the epidermis is thus:

$$R_{ss} = \frac{\rho_{saline}}{4r_{LDR}} \quad (3)$$

$$R_{se} = \frac{\rho_{epi}}{4r_{LDR}} \quad (4)$$

In the following analysis, we analyze the effect of exponential voltage pulses with time constants of $\tau_{pulse} = 1$ and 10 ms. In this case, the voltage applied across the tissue is:

$$U(t) = U_0 \exp(-t/\tau_{pulse}) \quad (5)$$

where τ_{pulse} is the pulse time constant. The model is, in fact, applicable to other pulse shapes; however, for the sake of brevity, our attention is focused on the commonly used exponential pulses.

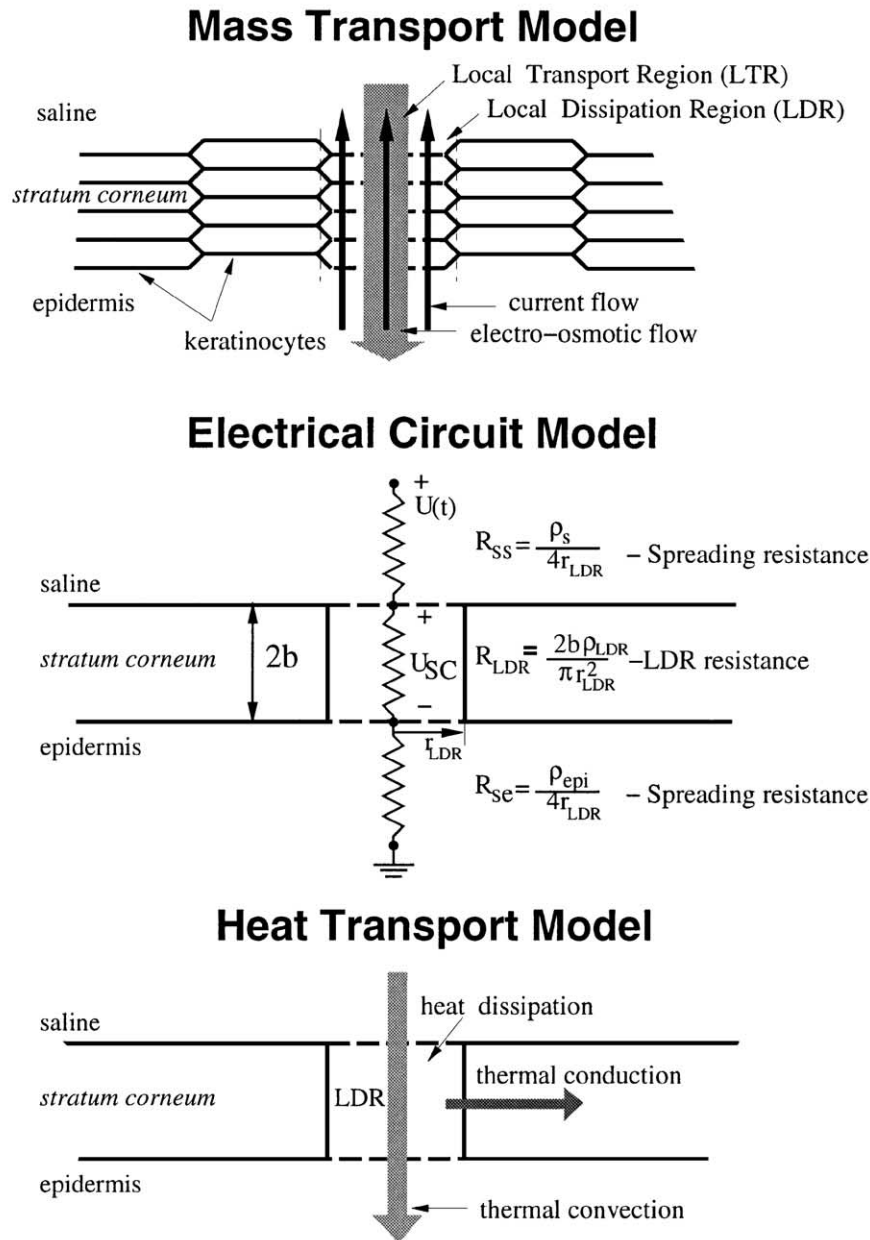


Fig. 2. Schematic model of the mass transport, current flow and heat transfer within an LDR/LTR in the stratum corneum during electroporation.

2.2. Thermal model

Once the electrical energy is dissipated into heat energy, it is transported by means of thermal conduction and convection. Conduction, as described macroscopically by the Fourier Law, is the transport of thermal energy by the random collisions of molecules, i.e. diffusion. Convection is the transport of thermal energy by the bulk motion of mass in a flow field [12]. In physiologic tissue, mass flow is always present in the form of blood flow through the vasculature. However, in the skin, the nearest capillaries are located in the dermis about 100 μm from the SC. Given the distance of these vessels from the LDR,

and the short time constant of the electrical pulse (10 ms or less), the effect of blood flow on the heat transfer is expected to be small and for the purposes of this analysis, is neglected.

During electroporation, it is possible for the pulse to induce the flow of aqueous fluid through pathways in the SC by osmosis, pressure and/or electro-osmosis. This flow will carry heat energy and thus cool the SC by thermal convection. Since the nature and magnitude of this flow field are not well understood, we undertake the analysis of two separate cases of heat transfer in the SC. The first case is the analysis of the pure thermal conduction problem where all flow is neglected. The second case is the analysis

of the thermal convection problem, which considers fluid flow through the SC and the resulting convective cooling. The first case analysis provides an estimate of the upper-bound temperature for the two pulsing protocol examples, while the second case analysis provides the lower-bound temperature rise.

2.2.1. Thermal conduction

Before proceeding with the computer thermal simulation of electroporation, it is instructive to estimate the order of magnitude of the temperature rise. Fundamentally, the peak, transient temperature rise is reached when the thermal energy storage is balanced by the electrical energy dissipation. In thermal analysis, the characteristic time and the characteristic linear dimension are important parameters, which, along with the thermal properties, govern the heat transport. For the case of exponential voltage pulses, the characteristic time is the time constant, τ_{pulse} , of the pulses. The characteristic length (d) is the length scale that incorporates most of the heated material. For this transient heat transfer process, the characteristic length is the larger of (1) the LDR radius (about 50 μm), and (2) the heat diffusion length ($\delta \approx \sqrt{\alpha \tau_{\text{pulse}}}$). If the thermal diffusivity (α) is assumed to be approximately equal to that of water (0.1 mm^2/s), then $\delta = 10 \mu\text{m}$. Therefore, we take the LDR radius as the characteristic length (d) and electrical energy dissipation is approximately:

$$Q \approx \frac{U_{\text{SC}}^2}{R_{\text{SC}}} \tau_{\text{pulse}} = \frac{U_{\text{SC}}^2 \pi r_{\text{LDR}}^2}{\rho_{\text{LDR}} 2b} \tau_{\text{pulse}}. \quad (6)$$

The balance of thermal energy with electrical dissipation gives:

$$\rho_{\text{M}} c \Delta T d^3 \approx Q = \frac{U_{\text{SC}}^2 \pi r_{\text{LDR}}^2}{\rho_{\text{LDR}} 2b} \tau_{\text{pulse}}. \quad (7)$$

Note that in Eq. (7) above, ρ_{M} is the mass density. Solving for temperature rise gives:

$$\Delta T \approx \frac{U_{\text{SC}}^2}{\rho_{\text{LDR}} 2b \rho_{\text{M}} c r_{\text{LDR}}} \tau_{\text{pulse}} \sim 20 \text{ } ^\circ\text{C}. \quad (8)$$

Typical experiments with $\tau_{\text{pulse}} = 1 \text{ ms}$ and significant molecular transport have $U_{\text{SC}} = 70 \text{ V}$, an LDR radius (r_{LDR}) of about 50 μm , a SC thickness ($2b$) of 15 μm and a thermal heat capacity ($\rho_{\text{M}} c$) that is about equal to that of water ($4.2 \times 10^6 \text{ J/m}^3$). For τ_{pulse} much less than the thermal relaxation time ($t_{\text{relax}} \sim r_{\text{LDR}}^2 / \alpha \sim 25 \text{ ms}$), the temperature rise is linear with the pulse time constant.

Using similar order of magnitude estimation, the temperature rise during single bilayer membrane electroporation can be approximated. In such a case, the transmembrane voltage, V , is transiently raised to about 1 V ($\tau_{\text{pulse}} \sim 1 \text{ ms}$) to create a single aqueous pathway with a diameter, a , (about 1 nm) through the membrane, (thickness, $L \sim 7$

nm). As with Eq. (7), the electrical energy dissipated in the pore is balanced by the energy stored and conducted, however in this case, the characteristic length, d , is equal to the heat diffusion length ($\delta \approx \sqrt{\alpha \tau_{\text{pulse}}}$).

$$\rho_{\text{M}} c \Delta T d^3 \approx \frac{V^2 a^2}{\rho_{\text{saline}} L} \tau_{\text{pulse}} \quad (9)$$

where ρ_{saline} is the resistivity of saline. The temperature rise is therefore:

$$\Delta T \approx \frac{V^2 a^2}{\rho_{\text{saline}} L \rho_{\text{M}} c (\alpha \tau_{\text{pulse}})^{3/2}} \tau_{\text{pulse}} \approx 5 \times 10^{-6} \text{ } ^\circ\text{C}. \quad (10)$$

Thus, temperature rise is expected to play a negligible role in membrane electroporation.

For the computer simulation of SC electroporation, the complete formulation of the Fourier heat conduction equation in the SC is used:

$$\rho(r, z) c(r, z) \frac{\partial T}{\partial t} = \nabla(k(r, z) \nabla T) + Q(r, z, t) \quad (11)$$

where T is the temperature rise above the baseline, $Q(r, z, t)$ is the power dissipation distribution in the LDR and in the surrounding saline and epidermis, $\rho(r, z)$ is the density, $c(r, z)$ is the specific heat and $k(r, z)$ is the thermal conductivity. The terms in Eq. (11) represent, from left to right, the thermal energy storage, the heat energy conducted, and the Joule heating from the electric field. Since the thermal system consists of materials of varying type, the thermal properties ($\rho(r, z)$, $c(r, z)$ and $k(r, z)$) are functions of space. The initial condition states that at time zero, the temperature rise everywhere is zero and the boundary conditions maintain that at infinite spatial extent, the temperature rise approaches zero.

Despite the simplifying assumptions, the governing equation (Eq. (11)) is a non-linear, transient partial differential equation in two dimensions. The solution of this type of equation is possible with the use of numerical techniques, namely the finite element method.

2.2.2. Thermal convection

The process of electroporation allows the transport of molecules across the SC. If there is an accompanying bulk motion of fluid through the aqueous pathways in the LDR, it will cause cooling by way of thermal convection. To estimate the order of magnitude of the temperature rise under such conditions, we assume that the electrical energy dissipated in the LDR is balanced with the heat energy transported by fluid motion of velocity u .

$$\rho_{\text{M}} c u \Delta T \pi r_{\text{LDR}}^2 \approx \frac{U_{\text{SC}}^2 \pi r_{\text{LDR}}^2}{\rho_{\text{LDR}} 2b} \quad (12)$$

$$\Delta T \approx \frac{U_{\text{SC}}^2}{\rho_{\text{LDR}} 2b \rho_{\text{M}} c u} \sim 20 \text{ } ^\circ\text{C}. \quad (13)$$

With the average, bulk fluid velocity, u , assumed to be equal to about 0.05 m/s, and using the same parameters as in Eq. (8), the temperature rise is about 20 °C. Note that this maximum temperature rise is independent of the pulse time constant. While at this point, the estimation of the bulk average fluid velocity seems arbitrary, we will motivate this assumption further below.

The governing equation which describes the temperature as a result of thermal convection is similar to Eq. (11), but Eq. (14) has the first term added to account for heat carried by the motion of the fluid through the aqueous pathways:

$$\rho_{MC} \vec{u} \cdot \vec{\nabla} T + \rho(r,z)c(r,z) \frac{\partial T}{\partial t} = \nabla(k(r,z)\nabla T) + Q(r,z,t) \quad (14)$$

where u is the fluid flow vector, ρ_{MC} is the saline heat capacity. The solution of Eq. (14) for temperature requires first that the fluid velocity field is known. For the flow of aqueous fluid through the pathways and into the epidermis, we model the tissue as a *porous medium* [12]. The porous medium model lumps together the complex flow patterns caused by a labyrinth of pathways into a flow continuum. Flow at each point in the field is not associated with any single pathway, but is considered to be an area-averaged, local flow in the media. This flow is solved from the continuity equation for an incompressible fluid with the appropriate boundary conditions.

In the aqueous pathways, the net flow direction is aligned with the z coordinate and there is no net flow in the r direction (see Fig. 1). For simplicity, we assume that the velocity u is constant in space, though u does depend on the time through its dependence on the voltage pulse. Outside of the LDR in the saline and the epidermis, fluid flow is modeled as inviscid and irrotational.

This bulk motion of the fluid through the LDRs is thought to primarily be the result of electro-osmosis [13]. In a pathway, the charged surface and the liquid electrolyte (saline) causes ions to preferentially gather near the pathway wall. The electric field from electroporation applies a force on the ions and causes net bulk fluid motion through the hydrodynamic entrainment of the saline electrolyte [14].

In order to model the thermal convection, it is necessary to estimate the magnitude of the electro-osmotic flow rate through the aqueous pathways. For fully developed flow, shear stress forces along the pathway wall balance the net forces on the electrolyte entrained in the ion motion. We model the aqueous pathways as tubes and solve for the average velocity due to electro-osmosis [14]:

$$u_p \approx \frac{-\varepsilon\Phi_s}{4\pi\mu} E_z \exp(-t/\tau_{\text{pulse}}) \quad (15)$$

where ε is the permittivity of the fluid, $E_z \exp(-t/\tau_{\text{pulse}})$ is the applied electric field along the tube, μ is the fluid viscosity, and Φ_s is the surface potential on the inside tube wall. The surface potential for an aqueous pathway with a

radius r_p through the SC has been calculated [15], which when combined with Eq. (15) gives the average velocity within the pathway:

$$u_p = \frac{E_z \exp(t/\tau_{\text{pulse}}) q}{\mu A_h} \left[\frac{1}{k} \frac{I_0(kr_p)}{I_1(kr_p)} \right] \quad (16)$$

where k is the inverse of the Debye length and I_0 and I_1 are the modified Bessel functions of the first kind of zeroth and first-order, q is the fundamental charge and A_h is the head area exposed to the pathway.

In order to estimate the magnitude of the electro-osmotic fluid velocity, the values listed in Table 1 are used in Eq. (16). These values give the approximate peak ($t \sim 0$) pathway fluid velocity to be 5 m/s. As mentioned above, the thermal, electrical and hydrodynamic properties associated with the LDRs in the model are determined from the pathway properties and the fractional aqueous area of the LDR. Thus, while the pathway fluid velocity is computed to be 5 m/s, the thermal convection model assumes the fluid convection to be lumped together over the entire LDR area. With a fractional aqueous area of about 1%, the area-averaged LDR fluid velocity is much smaller at 0.05 m/s.

This very simple model of the fluid motion due to electro-osmosis neglects (1) the complex and possibly tortuous geometry of the aqueous pathways, (2) the stochastic fluid and ion transfer through the 1-nm capillary and (3) the shielding of the surface potential by ions and bound water molecules. Despite these deficiencies, and in the absence of any experimental or theoretical analysis in the literature of flow through electroporated pathways, the model should provide an overestimate of the flow velocity.

For our study, NEKTON (Nektonics, Cambridge, MA) [16] was used to provide the finite element solution in both the thermal conduction and thermal convection analysis. Each of the FEM meshes contained 182 elements to solve the axisymmetric formulation of the problem with the axis of symmetry at $r=0$. Fifth-order polynomials were used as the trial functions and a time-step implicit solution scheme was used to solve the transient problem. The simulation ran on a Sun SparcStation X.

2.2.3. Thermal damage

Tissue damage during electroporation might occur by three possible mechanisms: (1) the temperature is high

Table 1
Parameters used to estimate the electro-osmotic velocity

Quantity	Symbol	Value	Reference
Pathway radius	r_p	10^{-9} m	[20]
Fluid viscosity	μ	0.823×10^{-3} N s/m ²	[21]
Electric field	E_z	5 V/ μ m	–
Debye length	$1/k$	10^{-9} m	[15]
Fundamental charge	q	-1.6×10^{-19} C	[22]
Head group area	A_h	4×10^{-19} m ²	[23]

enough to cause phase change in the SC lipids, (2) the temperature is high enough to cause phase change in the water such that the tissue is disrupted, or (3) the thermal time exposure exceeds a threshold such that cell death in the epidermis occurs. The concept of “damage” within the SC is not straightforward since the SC is comprised of non-living bilayer lipid membranes. Clearly, however, the SC has a physiologic function as a component of skin, and the skin might be considered to be damaged should that barrier function be chronically impaired. While the onset of phase change is easily recognized from the achieved temperature, the occurrence of cell death by thermal injury is modeled as a function of the temperature–time history.

The temperature–time exposure models the total accumulated injury to a tissue. It has been found [17] that the injury to skin was well described by the first-order rate:

$$\frac{d\Omega}{dt} = \Gamma \exp\left(-\frac{E}{RT}\right) \quad (17)$$

where Ω is an arbitrary measure of the degree of injury, Γ is a rate constant, E is an activation energy, R is the molar gas constant, and T is the absolute temperature. The parameters Γ and E are experimentally found for each different tissue type such that $\Omega=0$ for no injury and $\Omega>0$ for observable tissue damage (Table 2). The accumulated damage is determined by the integral of Eq. (17) over t_h , the time the tissue temperature is raised [17].

$$\Omega = \Gamma \int_0^{t_h} \exp\left(-\frac{E}{RT}\right) dt. \quad (18)$$

The onset of thermal damage for skin occurs when Ω is greater than 0.53 [17]. This model is used within the epidermis in conjunction with the thermal conduction and convection analysis to determine the potential thermal damage of an electroporation pulsing protocol.

Table 2
Parameters used in the thermal simulations

Quantity	Symbol	Value	Reference
LDR radius	r_{LDR}	50 μm	[4]
Saline resistivity	ρ_{saline}	0.72 $\Omega \text{ m}$	[22]
Epidermis resistivity	ρ_{epi}	26.3 $\Omega \text{ m}$	[17]
LDR resistivity (effective)	ρ_{LDR}	72 $\Omega \text{ m}$	–
SC voltage	U_{SC}	70 V	–
Saline thermal conductivity	k_{saline}	0.623 W/m K	[22]
Lipid thermal conductivity	k_{lipid}	0.209 W/m K	[24]
LDR thermal conductivity	k_{LDR}	0.209 W/m K	[24]
Epidermis thermal conductivity	$k_{\text{epidermis}}$	0.209 W/m K	[24]
Saline thermal diffusivity	α_{saline}	$1.5 \times 10^{-7} \text{ m}^2/\text{s}$	[22]
Lipid thermal diffusivity	α_{lipid}	$0.5 \times 10^{-7} \text{ m}^2/\text{s}$	[24]
Epidermis thermal diffusivity	$\alpha_{\text{epidermis}}$	$0.5 \times 10^{-7} \text{ m}^2/\text{s}$	[24]
Activation energy	E	244.0 kJ/mol	[17]
Rate constant	Γ	$2.9 \times 10^{37} \text{ 1/s}$	[17]
Molar gas constant	R	8.3143 J/K mol	[22]

3. Results and discussion

Fig. 3 summarizes the simulation results for both the conduction and the convection models. The top panel shows the peak temperature rise resulting from an exponential pulse, $\tau_{\text{pulse}} = 1 \text{ ms}$, for thermal conduction alone (solid line) and thermal convection (dashed line—fluid velocity of 1 m/s, dashed–dotted line—fluid velocity of 5 m/s). This peak temperature rise is taken at the center of the LDR ($z=0$, $r=0$) where the temperature is greatest at any given time. In the case of conduction alone, the peak temperature rise (about 19 °C) represents an upper-bound estimate of the rise that occurs during electroporation with a 1 ms pulse. The bottom panel of Fig. 3 correspondingly shows the temperature rise from a 10 ms pulse for both the conduction and the convection models. This example clearly shows the effect of a longer pulse on increasing the peak temperature rise.

Using Eq. (18) with the computed temperature–time history, the spatial extent of the thermal damage from a single pulse is quantified. With this model, the 1 ms pulse protocol showed no thermal damage from the integrated temperature history in the epidermis. The 10 ms pulse protocol, however, did give rise to a small amount of predicted thermal damage. Fig. 4 is a contour plot consisting of a single trace around the region of thermal damage from a single 10 ms pulse. The region of thermal damage is predicted to include an area in the center of the LDR and to extend about 5 μm into the epidermis. Subsequent pulses would have an additive effect on the predicted thermal damage. The application of this model, however, to tissue such as the SC, void of living cells, is questionable, since the model constants have been experimentally determined for living cells. In any event, the predicted thermal damage on SC and epidermis is minimal. This is consistent with in vivo experiments using hairless rats [19], which showed minor, acceptable levels of tissue irritation.

As expected from both the conduction and the convection models, the 1 ms pulse protocol causes a minimal temperature rise, no water phase change and no thermal damage in the epidermis. Also, the peak temperature rises above the in vivo baseline are smaller than the endothermic phase transitions for human SC (65, 80, and 95 °C [18]). However, for the 10 ms pulse protocol, the heating is more significant. The conduction model predicts a peak temperature rise, on top of the in vivo baseline, that is close to the water phase transition temperature and greater than the SC lipid transition temperatures.

Since electroporation has recently been experimentally found to induce mass transport through the SC, it is likely that thermal convection plays a major role in maintaining the SC temperature below the water vaporization point. The approximation of the flow magnitude from electro-osmosis (5 m/s peak fluid velocity) probably overestimates the true flow since this approximation neglected the shielding of the surface potential by bound water molecules and the complex

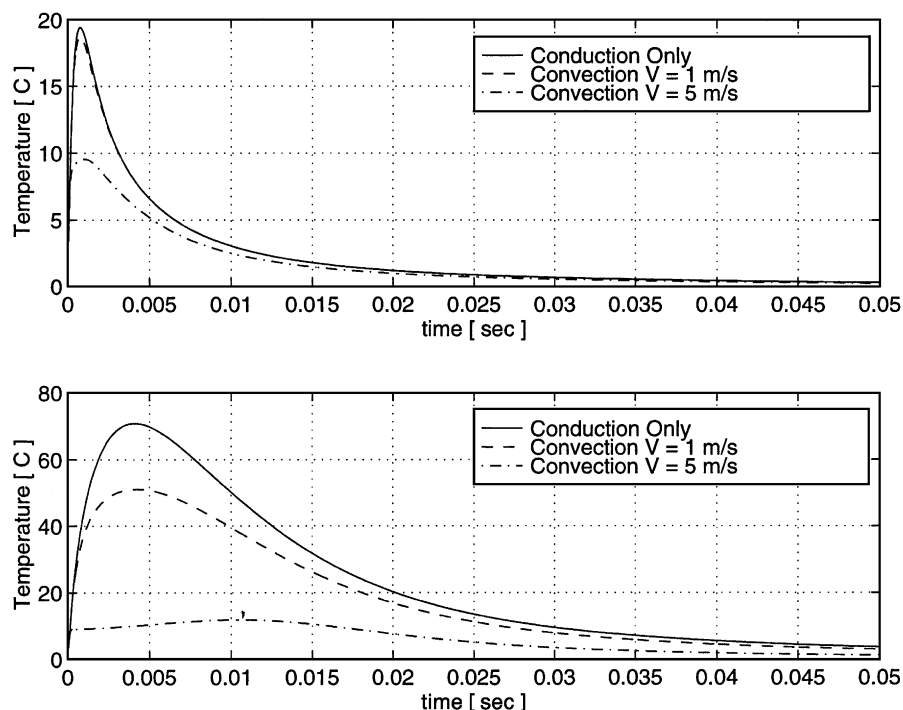


Fig. 3. Temperature rise as a function of time as computed from the thermal model for an LDR with a radius of 50 μm and $U_{\text{SC}} = 70$ V. The top panel, which contains results from 1 ms pulses, shows the temperature rise that results from the conduction model only (solid line) and the convection model (dashed lines) with peak fluid velocities of 1 and 5 m/s. The bottom panel contains the corresponding results but for a 10 ms pulse.

and possibly tortuous geometry of the aqueous pathways. The peak flow value of 1 m/s, also used in the simulation, was estimated from [13], which measured the total amount of tritiated water transported across the SC in vitro during electroporation. Additionally, in vivo studies of skin electroporation, with pulse durations up to 500 ms, showed little to no macroscopically observable damage in hairless rats [19], thus it is likely that the thermal convection that occurred during this protocol maintained the SC temperature at an acceptable level.

A limitation in the analysis is that both models do not consider the effect of phase change on the temperature rise. The enthalpy of phase change for the lipid and water substances would require energy that would otherwise go to increase the local temperature. Phase change can be, of course, accompanied by a change in the substance density, thermal properties and electrical properties. These may contribute to important secondary processes associated with the high voltage pulsing of skin. The rapid expansion of water, for instance, could disrupt the mechanical integrity of the tissue, change the electrical conductivity and change the thermal conductivity. It is not clear what the net effect of these non-linear processes would be on the tissue. Clearly, they would limit the temperature rise, but may increase the total damage to the tissue.

In the viable epidermis, the ensuing thermal damage as a result of the temperature–time history for the conduction model is shown in Fig. 4. This model computes the

maximum temperature rise and thus, it provides an upper-bound for the extent of the thermal damage which appears to be minimal and confined to the top 10 μm just below the LDR. Thus, for the 1–10 ms pulse protocols, there should be little to no thermal damage to the living cells. However, since the model does not consider the effects of phase change, some minor disruption of the SC may be possible by disruption of the tissue through water and lipid phase change.

The prediction of the temperature rise is directly dependent on the model for the dissipation of electrical energy in the LDR. The governing parameters of the dissipation include the voltage across the SC, U_{SC} , the resistance of the LDR, R_{LDR} , the thickness of the SC, $2b$, and the radius of the LDR, r_{LDR} . Together, these parameters form the energy dissipated per unit time per unit volume within the LDR as the internal heat generation. Dimensional analysis of the thermal conduction model reveals that the temperature rise is directly proportional to the internal heat generation per unit volume. Thus, for instance, in the approximation that other resistances do not limit the current flow, a doubling of the LDR resistance will result in a halving of the temperature rise. Furthermore, a doubling of the SC voltage will result in a quadrupling of the temperature rise. The dimensional analysis allows the results presented above to be applied to other pulsing protocols which have different parameters.

Dimensional analysis also reveals the relationship between the uncertainty in the parameters and the uncertainty

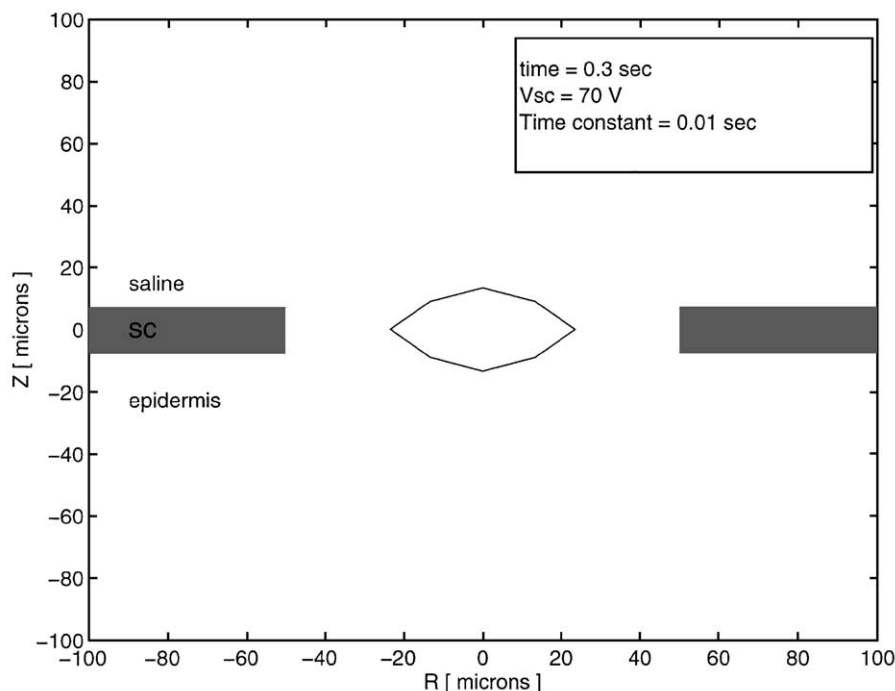


Fig. 4. Contour around the area of thermal damage for the thermal conduction model for an LDR with a radius of 50 μm , $U_{\text{SC}} = 70 \text{ V}$, and a pulse time constant of 10 ms. The damage region extends only slightly into the viable epidermis.

in the temperature rise prediction. In particular, the most variability is expected to be found in the size of the LDRs and the LDR resistance. In the present analysis, LDR resistance is estimated from the fractional aqueous area of electroporated skin. From sample to sample (0.7 cm^2 area), however, a fair amount of variability in skin resistance has been found (50–2000 Ω during pulsing [5]. The mechanisms that determine $F_{\text{w,ions}}$ are not fully understood, but it is believed to increase with the pulse time constant and pulse magnitude. Also, it is not fully understood how the LDR radius depends on the pulsing parameters, but a longer pulse tends to create larger LDRs [4]. These two effects will influence the temperature rise: the decrease in R_{LDR} from the increase in $F_{\text{w,ions}}$ will increase the temperature rise, however, the larger LDRs will have more volume over which the electrical energy is dissipated and decrease the temperature rise. It is unclear what the net effect on the temperature rise will be and therefore further experimental characterization of the LDR formation is needed before further temperature predictions can be made.

The question may be raised as to whether the increase in SC permeability to macromolecules during electroporation is fundamentally a thermal or an electrical phenomenon. While it is clear that electroporation causes a rapid decrease in the SC electrical resistance (increase in permeability to small, charged ions), it might be hypothesized that the associated increase in permeability to larger macromolecules is the result of a further, secondary morphological transformation caused by the SC temperature rise. A high enough temperature rise could disrupt the structure of the SC and hence its

normal barrier function by water vaporization and/or endothermic transformation of the lipids. Evidence against this hypothesis is given by the in vitro studies [2,4], that have shown the transport of fluorescently labeled macromolecules as the result of 1 ms duration pulses. As predicted by our thermal models presented here, the transdermal voltage and duration of these pulses would give rise, at most, to a 19 $^{\circ}\text{C}$ temperature rise. Such a transient temperature rise, on top of normal physiologic baseline, would not transform the SC and would not thermally alter its' permeability.

Furthermore, the aqueous pathways through the SC that exist even before the onset of electroporation are thought to be about 1 nm in radius [20]. When 70 V is applied across the skin, and just before the onset of electroporation, current flows through these pre-existing pathways. Another hypothesis is that heating from current flowing through the pre-existing pathways, before the onset of electroporation, can cause a change in the SC structure and increase the permeability to small ion transport. It is possible to estimate the magnitude of the temperature rise in such a case. Using Eq. (6), modified with the 1 nm radius aqueous pathway and assuming the fluid in these pathways has the same resistivity as saline, the peak temperature rise is estimated to be only about 0.001 $^{\circ}\text{C}$. According to this analysis, for the temperature rise in any pre-existing pathways to be larger than the 70 $^{\circ}\text{C}$ SC phase transition, the radius of such a pathway would have to be at least 65 nm. Such a pre-existing pathway of this size is not known to exist in the SC and therefore thermal phenomenon cannot be fundamental to electroporation. Rather, the thermal effects are subsequent to

the permeability increase caused by the electrical effects of electroporation.

4. Conclusion

Tissue electroporation holds promise as a mechanism for transdermal drug delivery. Of the many studies performed to date, very little attention has been given to the thermal effects that may be induced by these high voltage pulses. In this study, we have performed analytical and computer modeling of the temperature rise in the stratum corneum (SC) during electroporation. Current flowing through aqueous pathways created by electroporation dissipates electrical energy into heat energy. It is the purpose of this study to determine if the temperature rise in the SC might be large enough to thermally alter the barrier function of the SC, thermally damage cells in the nearby viable epidermis, and thermally alter any therapeutic molecules that are destined for transdermal transport across the SC.

The heat that is generated in the SC local dissipation regions (LDRs) is transferred by thermal conduction and by the thermal convection. Convective cooling is induced by the mass transport of water and other molecules across the SC. In one thermal model, conduction alone is considered in order to determine a maximum temperature rise. It was shown that for a peak voltage of 70 V applied across the SC with an exponential decay (1 ms time constant), the peak temperature rise was estimated to be 19 °C by the computer simulation, and 20 °C by the simple order of magnitude estimate. Thus, for the short 1 ms pulses, the temperature rise is small enough to not play a significant role in the SC permeability increase during electroporation. For 10 ms time constant pulses, the conduction model predicts temperature rises that approach water vaporization point. Yet, due to the short time exposure at these higher temperatures, the predicted thermal damage to the viable tissue under the SC is negligible. In practice, this higher temperature is not likely achieved due to the mass transfer through the SC and the subsequent cooling by thermal convection. The thermal convection model, which more realistically models the entire heat transfer during electroporation, predicts that the peak temperature rise will be between 12 and 51 °C for the 10 ms pulses (Fig. 3) and furthermore, the time–history thermal damage is non-existent.

While these relatively simple thermal models are instructive, experimental confirmation of the predicted results is warranted. In spite of major experimental challenges, it has been shown that for electroporating pulses applied to ex vivo human skin [3], the temperature rise from 1 ms pulses was unmeasurable with either an infrared (IR) detector or a liquid crystal. In that study, the liquid crystal required a temperature rise of about 25 °C above ambient in order to register a measurement. Also, while their IR detector could resolve 0.1 °C, it measured an area-averaged temperature over the optical field of view. Using longer (100–300 ms) trans-

dermal pulses [19], observed no visible thermal damage in the skin of hairless rats that underwent an electroporation protocol. While more experimental studies are necessary, the available results and the present study indicate that electroporation can be applied without thermally altering or damaging intact skin.

Acknowledgements

Supported by NIH Grant ARH4921 and Whitaker Foundation grant RR10963. The authors would like to thank Dr. Timothy Vaughan for his insight, comments and assistance.

References

- [1] M.R. Prausnitz, V.G. Bose, R. Langer, J.C. Weaver, Electroporation of mammalian skin: a mechanism to enhance transdermal drug delivery, *Proc. Natl. Acad. Sci. U. S. A.* 90 (1993) 10504–10508.
- [2] U. Pliquet, J.C. Weaver, Transport of a charged molecule across the human epidermis due to electroporation, *J. Controlled Release* 38 (1996) 1–10.
- [3] M.R. Prausnitz, V.G. Bose, R. Langer, J.C. Weaver, in: E.W. Smith, H.I. Maibach (Eds.), *Percutaneous Penetration Enhancers, Electroporation*, CRC Press, Boca Raton FL, 1995.
- [4] U. Pliquet, T.E. Zewert, T. Chen, R. Langer, J.C. Weaver, Imaging of fluorescent molecule and small ion transport through human stratum corneum during high voltage pulsing: localized transport regions are involved, *Biophys. Chem.* 58 (1996) 185–204.
- [5] U. Pliquet, R. Langer, J.C. Weaver, Changes in the passive electrical properties of human stratum corneum due to electroporation, *Biochim. Biophys. Acta* 1239 (1995) 111–121.
- [6] U.F. Pliquet, T.E. Zewert, T. Chen, R. Langer, J.C. Weaver, Imaging of fluorescent molecule and ion transport through human stratum corneum during high-voltage pulsing: localized transport regions are involved, *J. Biophys. Chem.* 58 (1996) 185–204.
- [7] M.R. Prausnitz, J.A. Gimm, R.H. Guy, R. Langer, J.C. Weaver, C. Cullander, Imaging regions of transport across human stratum corneum during high voltage and low voltage exposures, *J. Pharm. Sci.* 85 (1996) 1363–1370.
- [8] T. Chen, R. Langer, J.C. Weaver, Skin electroporation causes molecular transport across the stratum corneum through local transport regions, *J. Invest. Dermatol. Symp. Proc.* 3 (1998) 159–165.
- [9] S.A. Freeman, M.A. Wang, J.C. Weaver, Theory of electroporation for a planar bilayer membrane: predictions of the fractional aqueous area, change in capacitance and pore–pore separation, *Biophys. J.* 67 (1994) 42–56.
- [10] J.C. Weaver, Y.A. Chizmadzhev, Theory of electroporation: a review, *Bioelectrochem. Bioenerg.* 41 (1996) 135–160.
- [11] J. Newman, Resistance for flow of current to a disk, *J. Electrochem. Soc.* 113 (1966) 501–502.
- [12] A. Bejan, *Convection Heat Transfer*, Wiley, New York, 1984.
- [13] U.F. Pliquet, G.T. Martin, J.C. Weaver, Kinetics of the temperature rise within human stratum corneum during electroporation and pulse high-voltage iontophoresis, *Bioelectrochemistry* 57 (1) (2002) 65–72, in this issue.
- [14] K.P. Tikhomolva, *Electro-osmosis*, E. Horwood, New York, 1993.
- [15] L. Ilić, Mechanical contributions to energy of pore formation. BS Thesis, Massachusetts Institute of Technology, Cambridge, MA, 1994.
- [16] Nektonics, NEKTON Version 2.7 Documentation, Cambridge, MA, 1991.

- [17] B.I. Tropea, R.C. Lee, Thermal injury kinetics in electrical trauma, *J. Biomech. Eng.* 114 (1992) 241–250.
- [18] C.L. Gay, R.H. Guy, G.M. Golden, V.H.W. Mak, M.L. Francoeur, Characterization of low-temperature (i.e., <65 °C) lipid transitions in human stratum corneum, *J. Invest. Dermatol.* 103 (1994) 233–239.
- [19] R. Vanbever, D. Fouchard, A. Jadoul, N. De Morre, V. Preat, J.-P. Marty, In vivo non-invasive evaluation of hairless rat skin after high-voltage pulse exposure, *Skin Pharmacol. Appl. Skin Physiol.* 11 (1998) 23–34.
- [20] S.M. Dinh, C.W. Luo, B. Berner, Upper and lower limits of human skin electrical resistance in iontophoresis, *AIChE J.* 39 (1993) 2011–2018.
- [21] J.H. Lienhard, A Heat Transfer Textbook, 2nd edn., Prentice-Hall, Englewood Cliffs, NJ, 1987.
- [22] R.C. Weast (Ed.), *CRC Handbook of Chemistry and Physics*, CRC Press, Boca Raton, FL, 1984.
- [23] B. Alberts, D. Brag, J. Lewis, M. Raff, K. Roberts, J.D. Watson, *Molecular Biology of the Cell*, 3rd edn., Garland, New York, 1994.
- [24] H.F. Bowman, E.G. Cravalho, M. Woods, Theory, measurement and application of thermal properties of biomaterials, *Annu. Rev. Biophys. Bioeng.* 4 (1975) 43–80.